Original Article

Study of limestone and mill scale as fluxing agents for the recovery of tin from slag concentrates

Daniel Mapa Clemente [1]*
Johne Jesus Mol Peixoto [2]
José Roberto de Oliveira [3]
Raphael Mariano de Souza [3]
Carlos Antônio da Silva [2]

Abstract

Tin-slags with significant Sn and ZrO_2 levels are stored in Brazilian smelters and present potential to provide a Sn alloy to the market without additional cassiterite mining, thus contributing to minimizing environmental and social impacts. Some of these slags contain occluded metallic phases, so improving coalescence and sedimentation conditions during pyrometallurgical processing could enhance the recovery of Sn from these sources. However, critical information for process optimization, such as the melting temperature and viscosity of high ZrO_2 slags, is scarce. This research measured the melting temperatures of these slags using a softening and melting microscope under air atmosphere and used models to infer their viscosity. Based on results and optimization studies, the addition of mill scale and limestone as fluxes was proposed. The aim was to modify the properties of the slag, enhancing the recovery of Sn as a metallic button. The recovery of Sn as a metallic button was achieved at 1573K using combined additions of limestone and mill scale, but with a limited yield. Magnetic separation, which was used as an auxiliary technique, effectively retrieved most occluded metallic particles, even at 1473K.

Keywords: Tin; Melting temperature; FeSn; Tin slags.

1 Introduction

Tin (Sn) is a metal with high value and is used in various applications [1]. Its only economically viable ore is cassiterite [2,3], whose main reserves are in China, Indonesia, Burma, Australia, and Brazil [4]. Cassiterite mining in Brazil can occur in regions with the presence of conservation units and may lead to environmental impacts [5]. Examples are erosion and inappropriate discharge of tailings [3], the use of environmentally concerning reagents for flotation [6], among others. Furthermore, Sn ore is considered a conflict mineral, and its supply chain can be associated with social risks [7,8]. To minimize risks and impacts, it is crucial to optimize the recovery of Sn from secondary sources, producing more alloy without additional mining. According to Li et al. [9], this is an important approach to increase the lifetime of primary resources. Besides, Su et al. [10] reported that Sn reserves are running out, and secondary sources will become the main form of extracting Sn in the future.

Previous works have shown the origin of tin-slags. It should also be noted that primary tin-slags obtained during the reduction of cassiterite can be further processed, if necessary, to recover more Sn, and limestone is used as a flux in each processing step [2,11,12]. It can be inferred that components present in the cassiterite that are not easily reduced tend to be enriched in the slag. Up to around 20% ZrO_2 were measured in Brazilian slags [13,14], indicating this oxide could significantly influence its properties. Since stocks of high ZrO_2 tin-slags were reported at least in smelters in the states of São Paulo [14] and Rondônia [15], this could be an opportunity to increase the output of Sn without incurring the mentioned risks.

Clemente et al. [11] investigated occluded metallic phases in similar slags. They verified that these phases consisted of FeSn alloys that did not separate to the bottom of the furnace during the pyrometallurgical process. Thus, these were dragged by the final slag (named "end-slag" by these authors). Their research highlighted a lack of thermodynamic data concerning high ZrO_2 tin-slags but indicated that these exhibit high melting temperatures, potentially contributing to the loss of Sn. While conducting recovery experiments, they verified that a greater addition of limestone led to a higher coalescence of metallic

[1]*Laboratório de Pirometalurgia e Simulação - LAPSIM, Universidade Federal de Ouro Preto - UFOP, Ouro Preto, MG, Brasil.*
[2]*Departamento de Engenharia Metalúrgica e de Materiais, Universidade Federal de Ouro Preto - UFOP, Ouro Preto, MG, Brasil.*
[3]*Departamento de Engenharia Metalúrgica e de Materiais, Instituto Federal de Educação, Ciência e Tecnologia do Espírito Santo - IFES, Vitória, ES, Brasil.*

**Corresponding author: daniel.clemente@aluno.ufop.edu.br*
E-mails: johne.peixoto@ufop.edu.br; jroberto@ifes.edu.br; raphael.mariano10@gmail.com; casilva@em.ufop.br

particles, but even with an addition of 45% limestone, some metallic prills were still dragged by the end-slag.

Based on this information, the present research studied the use of mill scale and limestone as fluxing agents for the pyrometallurgical recovery of Sn from these tin-slags. It was aimed at enhancing processing conditions by promoting a higher level of coalescence of metallic particles. For this research, the melting temperature of the tin-slag was determined, and process optimization studies were carried out. Then, recovery experiments with a carbon resistance furnace were performed at 1573-1473K, and slag melting temperature measurements were conducted to support the results.

2 Materials and methods

This research employed tin slag concentrate, mill scale, and limestone as process inputs. This section presents the material description, characterization methods, theoretical studies, and the procedures used for melting temperature determination and pyrometallurgical experiments.

2.1 Materials

The tin-slag concentrate was provided by a Brazilian tin smelter with grain size <0.5 mm and was initially studied by Clemente et al. [11], who obtained it by concentrating Sn in the slag using a jig. Some slag/non-magnetic fractions generated in that earlier work were also made available for the present study.

In particular, the non-magnetic fraction of the tin-slag concentrate, referred to as the "oxidized phase of the concentrate" in the previous study, is of special relevance here: it represents the slag without metallic prills, which will be diluted by the proposed fluxing agents.

Mill scale and limestone (calcitic) were investigated as fluxing agents, and their composition is available in Table 1.

Mill scale is a by-product of the steelmaking process and consists mostly of Fe, in addition to contaminants such as Si, Mn, and Al, among others. Fe is found as FeO, Fe_3O_4, and Fe_2O_3, FeO being the major phase present [16,17].

2.2 Methods

2.2.1 Characterization and chemical analyses

Characterization of the concentrate was initially performed by Clemente et al. [11] and consisted of analyses by iodometric titration for Sn, energy dispersive X-ray fluorescence (EDXRF), microanalyses in a scanning electron microscope (SEM), and by an automatic mineralogical analysis system (TIMA-MIRA). These are briefly presented in the results section for better understanding. End-slags, non-magnetic fractions, magnetic fractions, as well as metallic buttons obtained in the current research were analyzed by iodometric titration for Sn (using the methodology reported by Price and Smith [18]) and by EDXRF. For the EDXRF, pressed pellets were prepared using samples ground in a planetary mill, passed through a 0.074 mm sieve, and pressed under a load of 20 t for 10 s. The equipment used was an Epsilon 3XL device from Malvern Panalytical. Slags were quantified as oxides, and results were normalized, except for the %Sn, which was determined via iodometric titration.

2.2.2 Melting temperature measurements

Melting temperatures of various slags/non-magnetic fractions were measured under an air atmosphere using a softening and melting microscope from Ernst Leitz GmbH, located at the Pyrometallurgy and Simulation Laboratory at UFOP (LAPSIM). The slag sample, ground below 0.074 mm, was pressed to form a cylinder with a diameter and height of 3mm, using alcohol as a binder. A digital camera follows the shape evolution of this cylinder under a heating rate of 10 K/min until 1073K, and 5 K/min thereafter. The melting point is visually identified when the height of the sample reaches 50% of its original size [19,20], according to the hemisphere method. Further details from the experimental setup were presented in another research [19].

The initial experiments in this study utilized different non-magnetic fractions previously generated by Clemente et al. [11], which originated from tests with additions of limestone ranging from 0 to 45 wt%. These non-magnetic fractions consist of high ZrO_2 tin-slags diluted with different additions of limestone and without metallic prills. After the pyrometallurgical experiments for Sn recovery performed in the present study, which used mill and scale and limestone as fluxing agents, the obtained non-magnetic fractions were also subjected to melting temperature measurements.

2.2.3 Theoretical studies aiming process optimization

FactSage 8.0 was used to assess the influence of additions of CaO and FeO on the melting temperature of the slag phase. For this, FToxid and FactPS databases were utilized.

The viscosity of the non-magnetic fraction from the concentrate from Clemente et al. [11] was assessed through the models of Urbain, Riboud, Iida, and optical basicity.

This was necessary since viscosity measurements of tin-slags with high ZrO_2 are unavailable. Besides, the viscosity modulus of FactSage 8.0 does not present data on ZrO_2. The viscosity expressions are from Eisenhuttenleute [21]

Table 1. Chemical composition (wt%) of limestone and mill scale analyzed by EDXRF

	$CaCO_3$	SiO_2	Al_2O_3	MnO	FeO	Others
Limestone	98.8	0.5	0.1	< 0.1	0.1	0.2
Mill scale	-	2.8	1.1	0.7	95	0.4

for Urbain and Riboud models, and from Iida et al. [22] for Ida´s model. Optical basicities were extracted from Mills et al. [23], Duffy [24], and Mills [25]. Divergences regarding the role of ZrO_2 and other oxides in the formation/modification of the slag, as well as their impact on these models, were reported by Clemente et al. [26]. Thus, to minimize errors, the average value from these models was taken for these analyses. Finally, the influence of additions of CaO and FeO on the viscosity of the oxidized phase was also studied using these models.

2.2.4 Pyrometallurgical experiments for the recovery of Sn

A 40 kVA carbon resistance furnace made by Ruhrstrat and located at the LAPSIM (UFOP) was used for pyrometallurgical experiments. In this furnace, the entire thermal cycle is performed under nitrogen atmosphere, and the sample is kept inside a graphite crucible. Samples were kept at the test temperature for 45 min, which was maintained with an accuracy of ± 5 K. Further details from the experimental setup were presented in previous research [11].

Different additions of mill scale, as well as combined additions of limestone and mill scale, were studied. All inputs were individually ground below 0.5 mm in a decontaminated planetary mill. For each experiment, inputs were sampled using a Jones Riffle Splitter and kept in a muffle at 373K for 48 h. Then, they were weighed in an AD330 semi-analytical balance from Marte, mixed, and placed in a graphite crucible. Table 2 details the temperatures, burdens, main test objectives, fluxes, and indicates which end-slags were magnetically separated. The percentage of each addition was calculated in relation to the mass of the concentrate.

Clemente et al. [11] found that even though the addition of limestone did not effectively lead to the recovery of Sn as a metallic button, it improved coalescence conditions, in some cases resulting in partially formed buttons found in the bottom of the crucible. These findings suggest that enhanced coalescence conditions could imply higher recovery of Sn as a metallic button. Based on this reasoning, the coalescence was assessed in tests A-I in the present study. For this, the end-slag from each test was gradually ground down to 1.7 mm using a mortar, while occluded metallic particles were retrieved by magnetic separation (with a neodymium magnet with 5300 Gauss). Then, alloy size distribution curves were plotted and compared. Considering the best achieved coalescence conditions, the recovery of Sn as a metallic FeSn button was investigated in tests J, K, and L.

Quantitative criteria to evaluate the Sn yield were established. In Equation 1, only the alloy obtained at the bottom of the crucible as a single metallic button was considered. When magnetic separation was applied, Equation 2 was used (both magnetic fraction and metallic buttons were considered).

$$Sn\,Yield\,(\%)_{metallic\ button} = \frac{Sn\,Mass_{(metallic\ button)}}{Sn\,Mass_{(concentrate)}} x100 \quad (1)$$

$$Sn\,Yield\,(\%)_{metallic\ button\ and\ magnetic\ fraction} = \frac{Sn\,Mass_{(metallic\ button,\ magnetic\ fraction)}}{Sn\,Mass_{(concentrate)}} x100 \quad (2)$$

3 Results and discussion

3.1 Characterization of the tin-slag concentrate

Table 3 shows the composition of the concentrate analyzed by Clemente et al. [11], revealing that it contains relatively high levels of Sn and Fe. Additionally, the presence of elements such as Si, Ca, Zr, Nb, and Al was verified. Also noteworthy is the high level of estimated %O, supporting the identification of the concentrate as a metal/slag mixture.

An analysis using the TIMA-MIRA system was performed by Clemente et al. [11], and has shown different metallic phases, such as Sn, Sn(Fe), and Fe(Sn). These are occluded inside oxidized phases such as Augite (Zr) and Slag (Fe,Sn), which have high values of estimated %O and different concentrations of Zr, Nb, Ca, Si, and Al, among other elements. The composition of this non-magnetic

Table 2. Experimental conditions of each test

Test ID	T (K)	Limestone (wt%)	Mill scale (wt%)	Main objective	Magnetic separation
A	1573	0	15	Study the influence of mill scale on the metallic coalescence	Yes
B	1573	0	30		Yes
C	1573	15	10	Study the influence of combined additions of limestone and mill scale on the metallic coalescence	Yes
D	1573	15	20		Yes
E	1573	15	30		Yes
F	1523	15	10		Yes
G	1473	15	10		Yes
H	1473	15	20		Yes
I	1473	15	30		Yes
J	1573	15	10	Study the influence of combined additions of limestone and mill scale on the recovery of Sn as a metallic button	No
K	1573	15	20		No
L	1573	15	30		No

fraction (oxidized phase of the concentrate) is presented in Table 4. It is highly complex and contains many oxides at significant levels, such as SiO_2, CaO, ZrO_2, Nb_2O_5 and Al_2O_3.

Using the methodology described in section 2.2.2, its melting point was determined in the current research as 1403K. This value is even below those described by Wright [2] for tin slags with much lower ZrO_2 content, which ranged from 1523-1673K. The determination process is presented in Figure 1.

3.2 Melting temperature and viscosity measurements and calculations

Clemente et al. [11] tested limestone additions varying from 0 to 45 wt%. The present research measured the melting temperatures of some slags from these authors and compared the results to predicted values from FactSage 8.0 (Table 5). The measured values significantly differ from the calculations, and certain factors aid in explaining these differences. Firstly, Sn is said to be lost in the slag as $SnO.SiO_2$ [2]. However, previous research [11] using FactSage estimated Sn to be present as SnO_2 (which has a high melting point of 1903K [27]). Furthermore, the software also identified relevant levels of Nb_2O_5 and Ta_2O_5 in the solid slag phases, which are also oxides with high melting points. However, the TIMA-MIRA analysis of the concentrate [11] indicated that oxides containing Nb and Ta tend to solidify together with oxides with Fe, Si and Al, which possibly lead to compounds other than Nb_2O_5 and Ta_2O_5. Thus, it is likely that the software didn't correctly identify the proper phases for such complex slags, leading to incorrect calculations. X-ray diffraction (XRD) analysis of the solidified slag could have helped to confirm the presence of crystalline Nb- and Ta-bearing phases other than Nb_2O_5 and Ta_2O_5, although the possible presence of amorphous phases must be considered. This analysis will be the subject of future studies. Finally, FactSage calculations were performed at iron saturation, while the melting experiments were performed under air atmosphere. Despite these divergences, there are two important conclusions: there is indication that melting temperatures of these slags are not as high as previously thought, and additions of up to 45% limestone do not significantly influence this property.

Considering these inconsistencies, FactSage 8.0 was used only to better understand the expansion of the fluid phase field by the addition of FeO. For this analysis, a $CaO.SiO_2.ZrO_2$ phase diagram is presented in Figure 2A, and this diagram has only a limited fluid region at 1773K. The composition of the oxidized phase of the concentrate (normalized for SiO_2, CaO and ZrO_2) lies outside the fluid region. Then, Figure 2B simulates a 30% FeO addition at 1773K, resulting in an expansion of the liquid area. The oxidized phase is almost inside this region, indicating a

Table 3. Composition (wt%) of the Sn concentrate (Clemente et al. [11])

Sn	Si	Fe	Ca	Zr	Nb	Ta	Al	Ti	Mg	Mn	P	Others	O (balance)
27.0	15.0	13.4	9.4	5.2	3.7	0.7	2.5	0.8	0.5	0.6	0.1	5.6	15.5

Table 4. Composition (wt%) of the oxidized phase of the concentrate (Clemente et al. [11])

SnO_2	FeO	SiO_2	CaO	ZrO_2	Nb_2O_5	Al_2O_3	TiO_2	MgO	Ta_2O_5	Others
0.5	2.0	46.0	15.8	11.3	6.9	6.5	1.4	1.4	0.9	7.1

Table 5. Melting temperatures of different slags

Test ID from Clemente et al. [11]	Addition of limestone	Melting temperatures calculated by FactSage (K)	Measured melting temperatures (K)
1	0%	1801	1403
2	15%	1701	1413
5	30%	1719	1378
6	45%	1770	1396

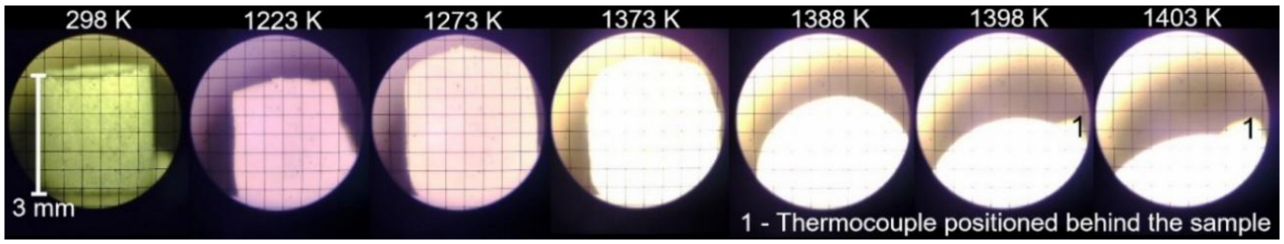

Figure 1. Melting temperature determination of the oxidized phase of the concentrate.

high level of liquid phase. Thus, based on this simplified study, it is hypothesized that additions of FeO could lead to better conditions for the coalescence of metallic particles.

Another important aspect is the impact of additions of CaO and FeO on the slag's viscosity. The role of CaO in the breakage of SiO_4^{4-} polymeric chains is well known, and this flux is normally used in tin metallurgy to reduce the slag's viscosity [2,21]. However, studies on the influence of FeO are unavailable for these slags. According to the viscosity models described in section 2.2.3, it is indicated that additions of CaO (Figure 3a) and FeO (Figure 3b) result in lower viscosity values. Naturally, this reasoning is valid for liquid slags only.

3.3 Influence of mill scale on the metallic coalescence (tests A-B)

Some larger metallic particles were found at the bottom of the crucible with an addition of 15% mill scale, and a clear metallic button was verified with 30% mill scale. However, even under this last condition, many metallic prills could be seen dispersed in the end-slag, indicating incomplete alloy removal. Magnetic separation was applied and metallic buttons, as well as magnetic fractions are presented in Figure 4. These were used to plot grain size distribution curves, in which can be observed that the level of coalescence is increased when compared to the original concentrate, as most particles are larger than 0.5 mm (maximum grain size of the concentrate). This indicates that the mill scale may enhance processing conditions at 1573K.

The metallic buttons and magnetic fractions were ground together and analyzed for each test. Results are presented in Table 6, revealing that these are FeSn alloys with high Sn content. As they can be used as input in other processes [2], they were accounted as a form of Sn recovery. The recovery levels of tests A and B, including magnetic separation, reached 89.2% and 90.8%, respectively.

Table 7 presents the chemical analyses of the non-magnetic fractions (obtained in tests which used magnetic separation) and end-slags (obtained in tests without magnetic separation) for all experiments, and it is noteworthy that higher SnO_2 levels were measured with an increase in mill scale (tests A and B).

Besides, it should be noted that the oxidized phase of the concentrate shown in Table 4 was melted without any

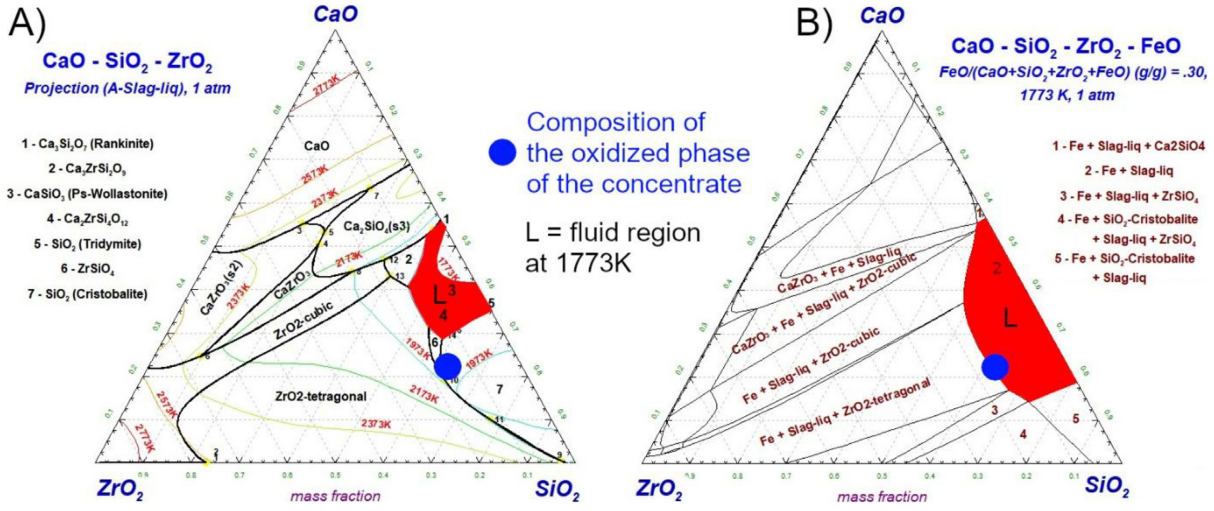

Figure 2. (A) $CaO.SiO_2.ZrO_2$ phase diagram (B) Influence of FeO on the presence of liquid slag at 1773K. Adapted from FactSage 8.0.

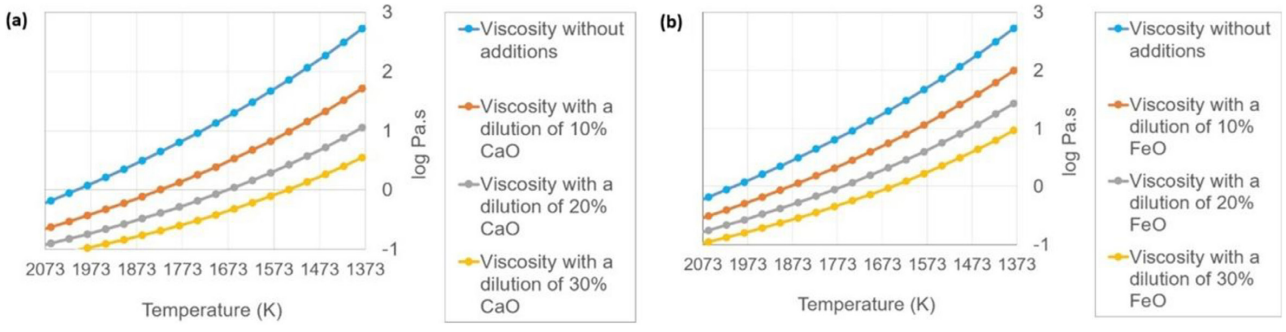

Figure 3. Influence of additions of (a) CaO and (b) FeO on the viscosity of the oxidized phase considering average viscosity values obtained using four models and liquid slags.

Figure 4. Influence of mill scale on the coalescence of metallic particles at 1573K (tests A and B).

Table 6. Chemical analyses (wt%) of magnetic fractions/metallic buttons

Test	T(K)	Sn	Fe	Nb	Si	Pb	Ca	Zr	Mn	Cu	Others
A	1573	58.9	38.0	0.1	0.7	1.0	0.3	0.1	0.1	0.2	0.6
B	1573	53.8	43.0	0.1	0.6	1.2	0.4	0.1	0.1	0.3	0.5
C	1573	61.1	35.4	0.1	0.7	1.2	0.5	0.1	0.0	0.2	0.7
D	1573	59.4	37.7	0.0	0.3	1.4	0.4	0.0	0.0	0.2	0.4
E	1573	57.8	39.2	0.1	0.2	1.4	0.5	0.1	0.0	0.3	0.4
F	1523	63.4	31.7	0.2	1.4	1.3	0.9	0.2	0.1	0.2	0.7
G	1473	64.2	28.9	0.2	2.4	1.2	1.5	0.4	0.1	0.2	0.9
H	1473	61.2	33.0	0.2	1.7	1.2	1.3	0.3	0.1	0.2	0.8
I	1473	59.0	37.7	0.1	0.7	1.1	0.5	0.1	0.0	0.2	0.6
J	1573	64.5	32.4	0.0	0.6	1.1	0.4	0.0	0.0	0.2	0.6
K	1573	61.9	35.5	0.0	0.0	1.4	0.3	0.0	0.0	0.3	0.5
L	1573	59.1	38.7	0.0	0.1	0.9	0.2	0.0	0.0	0.3	0.6

Table 7. Chemical analyses (wt%) of end-slags and non-magnetic fractions

Test	T(K)	SnO_2	FeO	SiO_2	CaO	ZrO_2	Nb_2O_5	Al_2O_3	TiO_2	MgO	Ta_2O_5	Others
A	1573	2.4	15.1	37.1	13.3	8.7	7.1	5.2	1.1	1.1	0.8	8.1
B	1573	2.7	26.9	30.4	10.9	7.5	6.0	4.1	1.0	0.9	0.7	8.9
C	1573	1.1	8.0	37.2	22.8	8.6	6.8	5.2	1.1	1.2	0.7	7.2
D	1573	1.9	18.3	31.8	19.7	7.4	5.9	4.4	1.0	1.1	0.6	7.9
E	1573	2.2	25.8	28.1	17.5	6.6	5.2	3.8	0.8	0.9	0.6	8.4
F	1523	1.7	12.3	34.8	21.6	8.1	6.4	4.8	1.0	1.1	0.7	7.4
G	1473	2.6	13.5	34.0	20.9	7.7	6.1	4.8	1.0	1.1	0.7	7.5
H	1473	2.9	21.6	29.7	18.6	6.8	5.5	4.3	0.9	1.0	0.6	8.2
I	1473	3.0	24.7	28.6	17.6	6.3	5.0	4.0	0.8	1.0	0.6	8.3
J	1573	10.7	10.6	34.1	19.2	6.2	4.8	4.9	1.0	1.2	0.6	6.6
K	1573	7.6	20.3	29.6	17.5	6.1	4.7	4.1	0.9	1.0	0.6	7.6
L	1573	6.1	22.7	29.0	17.2	6.0	4.7	4.0	0.9	1.0	0.6	7.9

flux and presented a level of only 0.5% SnO_2, reinforcing this inference. This suggests potential oxidation of Sn by mill scale, which is also supported by decreasing Sn content in the metallic buttons/magnetic fractions from tests A and B. A simplified reaction in Equation 3 between Sn/Fe and SnO/FeO provides a plausible explanation for this oxidation. In this context, higher additions of mill scale increased the FeO concentration, and consequently the residual level of SnO.

$$SnO_{(l)} + Fe_{(l)} = Sn_{(l)} + FeO_{(l)} \quad (3)$$

3.4 Influence of mill scale and limestone on the metallic coalescence (tests C-I)

Figure 5 illustrates that combined flux additions of mill scale and limestone enhanced the formation of metallic buttons at 1573K (tests C, D and E). Furthermore, metallic coalescence was mostly improved compared to individual mill scale additions. Increasing the amount of this last flux did not affect the distribution curves for grain sizes <5.6 mm.

However, it is visually apparent that the coalescence was improved for larger particles.

Interestingly, Sn levels in the alloy also diminished with more mill scale addition, but in this case, this possible oxidation effect seems to be less pronounced. For instance, with a 30% mill scale (test B), 53.8% Sn was measured in the metallic fraction, whereas with 10% limestone and 30% mill scale (test E), the measured Sn was 57.8%. A higher yield, ranging from 94.4% to 91.1%, was calculated for these experiments considering magnetic separation.

Based on these results and the relatively low melting temperatures presented in Table 5, experiments were extended to 1523K (test F) and 1473K (tests G, H and I). As shown in Figure 6A, temperature significantly influences metallic coalescence and the formation of a metallic button, when considering the same burden (in this case, 15% limestone and 10% mill scale). Additionally, it seems that with less coalescence, it is more difficult to separate metallic prills from the oxidized phase by magnetic separation. For instance, the magnetic fraction of test G, performed at 1473K and using the same burden, was contaminated with up to 4.3% of Ca, Si, and Zr, which are elements mostly present in the oxidized phase. For comparison, the sum of these elements in the alloy in test C (1573K) is only 1.3%. Despite this, the yield considering Equation 2 was high in any temperature and ranged from 93.1% at 1473K to 94.4% at 1573K.

Figure 6B, in which experiments were conducted at 1473K, illustrates a significantly lower coalescence compared to tests performed at 1573K. Even though increasing the mill scale addition also resulted in better coalescence conditions, the Sn yield with the use of magnetic separation was slightly lower and ranged from 90.9-93.1%.

Higher Sn losses can be attributed to the poor separation of metallic and oxidized phases, which are also supported by

Figure 5. Influence of limestone and mill scale at 1573K (tests C, D and E).

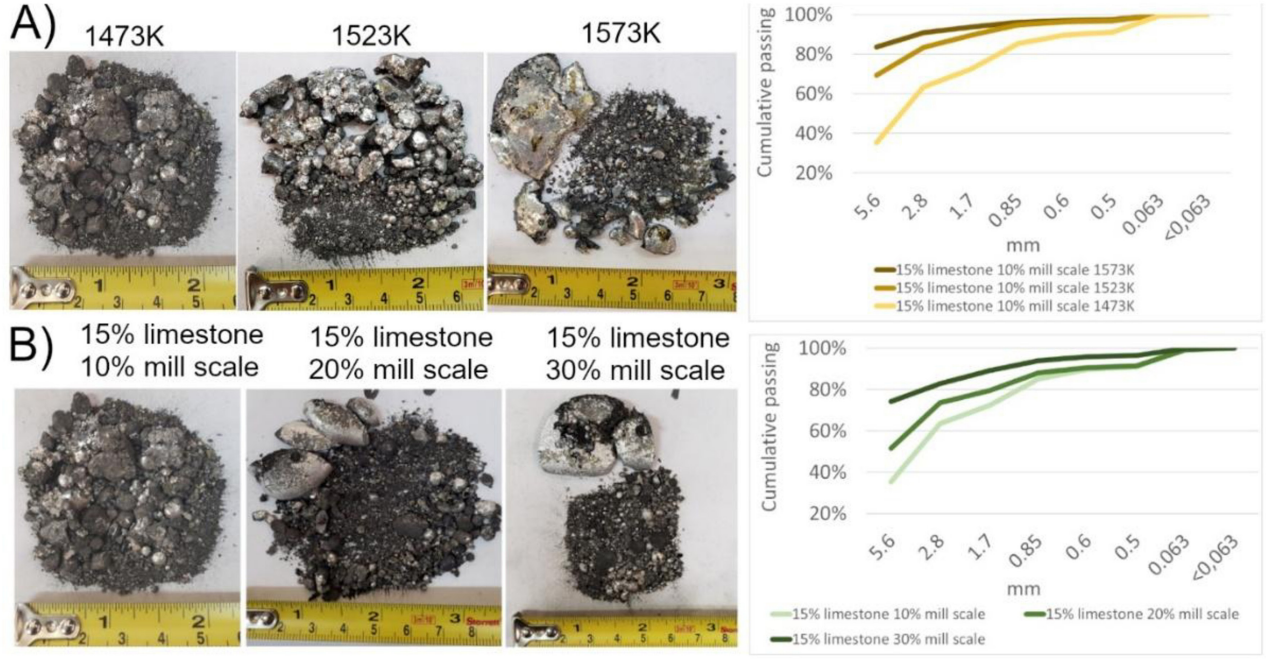

Figure 6. (A) Influence of temperature with a fixed addition of 15% limestone and 10% mill scale (tests G, F and C); (B) Influence of limestone and mill scale at 1473K (tests G, H and I).

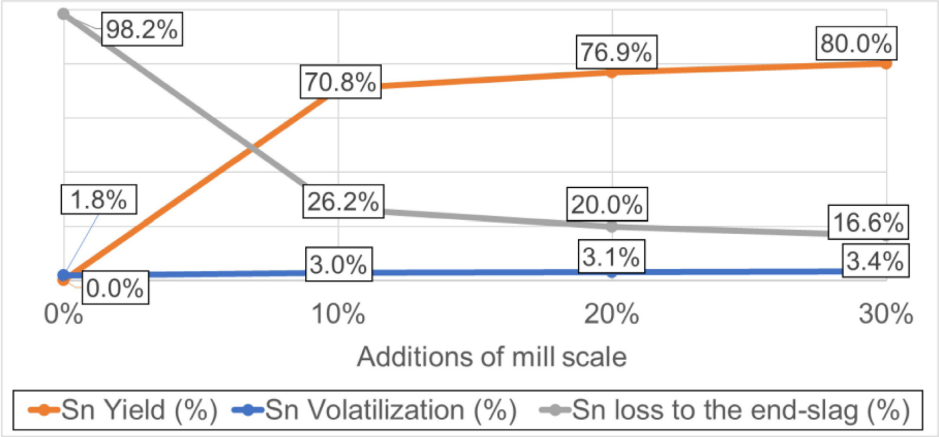

Figure 7. Recovery of Sn as a metallic button considering the best conditions.

Table 8. Melting temperatures measured for the non-magnetic fractions of tests A-E

Test	A (15% M, 0% L)	B (30% M, 0% L)	C (10% M, 15% L)	D (20% M, 15% L)	E (30% M, 30% L)
Tm (K)	1373	1449	1363	1373	1386

M - Mill scale addition; L - Limestone addition; Tm - Measured melting temperature.

greater SnO_2 levels in the non-magnetic fractions of these tests. A comparison between results from tests performed at 1573K and 1473K suggest that smelters can also opt to process concentrates with lower temperatures to minimize energy costs, while retrieving the metallic particles using magnetic separation with some slag contamination.

3.5 Influence of limestone and mill scale on the recovery of Sn as a metallic button (tests J-L)

Considering the best coalescence conditions, which were obtained at higher temperatures and with combined additions of mill scale and limestone, tests were conducted at 1573K to assess the recovery of Sn exclusively as a metallic button. Yields as high as 70.8% were obtained for 15% limestone and 10% mill scale, as shown in Figure 7, while further additions also enhanced the process. It is clearly indicated that the dilution of the slag with limestone and mill scale, as well as an increase in temperature favor the formation of a metallic button.

However, SnO_2 levels from end-slags from these tests surpassed those reported in the literature [2,11], which can be attributed to occluded metallic particles trapped in the slag, as demonstrated in previous sections. It is interesting to note that the recovery using magnetic separation is much higher when compared to the formation of a metallic button, even under enhanced conditions. Thus, it should be used by smelters as an auxiliary recovery technique.

3.6 Additional melting temperature measurements

To explain the increased coalescence and formation of metallic buttons, the melting points of slags from tests A-E, representing all proposed burdens, were also measured. As presented in Table 8, the melting points are below the experimental temperatures, and it is indicated that these slags were liquid during the experiments. Thus, it is possible that viscosity of the melt was diminished by additions of FeO and/or CaO and that due to increased mobility of metallic droplets, a greater level of collision between metallic particles may also have occurred, resulting in a higher coalescence level. However, this hypothesis should be further explored in future studies with actual viscosity measurements.

4 Conclusions

This research aimed to optimize Sn recovery from complex tin-slags with high ZrO_2 by improving coalescence of metallic droplets dispersed inside these slags. To achieve this, a tin-slag concentrate was characterized, slag's melting temperatures were determined, optimization studies were performed, and smelting experiments were conducted at 1573-1473K using limestone and mill scale as fluxes.

Characterization suggested that Fe and Sn are present mainly in metallic form and occluded in a complex oxidized phase, which has CaO, SiO_2, and ZrO_2 as its main components. The melting temperature of the oxidized phase, as well as of other slags from previous research were measured and results revealed lower temperatures than previously inferred. Optimization studies indicated that additions of mill scale and limestone could enhance process conditions by either expanding the liquid region and/or diminishing the viscosity of the melt.

The impact of mill scale additions was studied at 1573K and led to increased coalescence, while also favoring the formation of a metallic button. However, metallic prills

were still found in the end-slag and magnetic separation was employed, allowing a Sn yield ranging from 89.2% - 90.8%. Combined additions of mill scale and limestone were performed between 1573 - 1473K and the effect of adding both fluxing agents, as well as the influence of temperature on the coalescence conditions were evident. Once again, magnetic separation was highly efficient for all conditions and allowed a yield ranging from 94.4 - 91.1% at 1573K and 93.1 - 90.9% at 1473K. The recovery of Sn as a metallic button was investigated at 1573K, but the yield was limited to 70.8% - 80.1%.

At last, melting temperature measurements for all test conditions were performed and indicated that the slags were fluid during the experiments. Thus, it is possible that the viscosity of the slag was positively influenced by these additions. Due to its importance, this subject should be the focus of future studies for the recovery of Sn from these sources.

Acknowledgements

The authors would like to acknowledge the support of Conselho Nacional de Desenvolvimento Científico e Tecnológico (CNPq), Coordenação de Aperfeiçoamento de Pessoal de Nível Superior (CAPES) and Fundação de Amparo à Pesquisa do Estado de Minas Gerais (FAPEMIG).

References

1 Tin use [homepage on the internet]. St. Albans: International Tin Association; 2025 [cited 2025 Jul 13]. Available at: https://www.internationaltin.org/how-is-tin-used

2 Wright P. Extractive metallurgy of tin. 2nd ed. Amsterdam: Elsevier Scientific Publish Company; 1982.

3 Maia F, Veiga MM, Stocklin-Weinberg R, Marshall BG, Constanzo C, Hariojati N, et al. The need for technological improvements in Indonesia's artisanal cassiterite mining sector. The Extractive Industries and Society. 2019;6(4):1292-1301. https://doi.org/10.1016/j.exis.2019.07.010.

4 U.S. Geological Survey. Mineral Commodity Summaries. Tin. USA: U.S. Geological Survey; 2023 [cited 2025 Jul 13]. Available at: http://pubs.usgs.gov/periodicals/mcs2023/mcs2023-tin.pdf

5 Rudke AP, de Souza VAS, Dos Santos AM, Xavier ACF, Rotunno OC Fo, Martins JA. Impact of mining activities on areas of environmental protection in the southwest of the Amazon: a GIS-and remote sensing-based assessment. Journal of Environmental Management. 2020;263:110392. https://doi.org/10.1016/j.jenvman.2020.110392. PMid:32174531.

6 Angadi SI, Sreenivas T, Jeon HS, Baek SH, Mishra BK. A review of cassiterite beneficiation fundamentals and plant practices. Minerals Engineering. 2015;70:178-200. https://doi.org/10.1016/j.mineng.2014.09.009.

7 Organisation for Economic Co-operation and Development. OECD due diligence guidance for responsible supply chains of minerals from conflict-affected and high-risk areas. Paris: OECD; 2016 [cited 2025 Jul 13]. Available at: https://www.oecd.org/en/publications/oecd-due-diligence-guidance-for-responsible-supply-chains-of-minerals-from-conflict-affected-and-high-risk-areas_9789264252479-en.html

8 The European Commission. Conflict minerals regulation explained. Brussels: European Commission Trade Department; 2021 [cited 2025 Jul 13]. Available at: https://policy.trade.ec.europa.eu/development-and-sustainability/conflict-minerals-regulation/regulation-explained_en

9 Li H, Qin W, Li J, Tian Z, Jiao F, Yang C. Tracing the global tin flow network: highly concentrated production and consumption. Resources, Conservation and Recycling. 2021;169:105495. https://doi.org/10.1016/j.resconrec.2021.105495.

10 Su Z, Zhang Y, Liu B, Lu M, Li G, Jiang T. Extraction and separation of tin from tin-bearing secondary resources: a review. Journal of the Minerals Metals & Materials Society. 2017;69(11):2364-2372. https://doi.org/10.1007/s11837-017-2509-1.

11 Clemente DM, da Silva CA, Peixoto JJM, de Oliveira JR, de Souza RM. Investigation of the presence of metallic phases in Brazilian tin-slags. Journal of Materials Research and Technology. 2023;24:6861-6875. https://doi.org/10.1016/j.jmrt.2023.04.251.

12 Graf GG. Tin, tin alloys, and tin compounds. In: Ullmann's encyclopedia of industrial chemistry [E-BOOK]. Weinheim: Wiley-VCH; 2000. https://doi.org/10.1002/14356007.a27_049.

13 Brocchi EA, Moura FJ. Chlorination methods applied to recover refractory metals from tin slags. Minerals Engineering. 2008;21(2):150-156. https://doi.org/10.1016/j.mineng.2007.08.011.

14 Garcia MAA. Caracterização radioquímica e impacto radiológico ambiental no processamento de cassiterita para produção de Sn e chumbo metálicos [thesis]. São Paulo: Universidade de São Paulo; 2009.

15 Buch T, Marbler H, Haubrich F, Trinkler M. Investigation of tin and tantalum ores from the Rondônia Tin Province, northern Brazil, to develop optimized processing technologies [Internet]. Berlim: DERA Rohstoffinformationen; 2018. Vol. 37 [cited 2025 Jul 13]. 164 p. Available at: https://rigeo.sgb.gov.br/items/f6f19101-182a-4cf3-a780-16a7d16037fe

16 Cunha AFD, Mol MPG, Martins ME, Assis PS. Caracterização, beneficiamento e reciclagem de carepas geradas em processos siderúrgicos. Rem: Revista Escola de Minas. 2006;59:111-116. https://doi.org/10.1590/S0370-44672006000100014.

17 Bagatini MC, Zymla V, Osório E, Vilela ACF. Characterization and reduction behavior of mill scale. ISIJ International. 2011;51(7):1072-1079. https://doi.org/10.2355/isijinternational.51.1072.

18 Price JW, Smith R. Tin: handbuch der analytischen chemie/handbook of analytical chemistry. Vol. 3/4/4a/4a g. Berlin: Springer; 1978.

19 Clemente DM, Menezes RDOT, Damaso HV, Peixoto JJM, da Silva CA. Study of the compositional and melting characteristics of some Brazilian and Congolese tin slags. Revista Tecnologia em Metalurgia, Materiais e Mineração. 2024;21:e3061. http://dx.doi.org/10.4322/2176-1523.20243061.

20 Li J, Wang SJ, Xia YJ, Kong H. Study on dephosphorisation of hot metal pretreatment with Al2O3 to replace CaF2 in slag. Ironmaking & Steelmaking. 2015;42(1):70-73. https://doi.org/10.1179/1743281214Y.0000000213.

21 Eisenhüttenleute V. Slag atlas. 2nd ed. Düsseldorf: Verlag Stahleisen GmbH; 1995.

22 Iida T, Sakai H, Kita Y, Murakami K. Equation for estimating viscosities of industrial mold fluxes. High-Temperature Materials and Processes. 2000;19(3-4):153-164. https://doi.org/10.1515/HTMP.2000.19.3-4.153.

23 Iida T, Sakai H, Kita Y, Shigeno K. An equation for accurate prediction of the viscosities of blast furnace type slags from chemical composition. ISIJ International. 2000;40(Suppl):110-114. https://doi.org/10.2355/isijinternational.40.Suppl_S110.

24 Duffy JA. Optical basicity of titanium (IV) oxide and zirconium (IV) oxide. Journal of the American Ceramic Society. 1989;72(10):2012-2013. https://doi.org/10.1111/j.1151-2916.1989.tb06022.x.

25 Mills K. The estimation of slag properties. Short course presented as part of Southern African Pyrometallurgy 2011. 2011 [cited 2025 Jul 13]. Available at: https://www.pyro.co.za/KenMills/KenMills.pdf

26 Clemente DM, Silva CA, Oliveira MJM, Peixoto JJM. Recovery of tin from high ZrO2 tin slags. In: Anais do 51° Seminário de Fusão, Refino e Solidificação de Metais; 2022; São Paulo, Brasil. São Paulo: ABM; 2022. p. 367-380. https://doi.org/10.5151/2594-5300-34539.

27 Chen Z, Xu Z, Zhao H. Flame spray pyrolysis synthesis and H2S sensing properties of CuO-doped SnO2 nanoparticles. Proceedings of the Combustion Institute. 2021;38(4):6743-6751. https://doi.org/10.1016/j.proci.2020.06.315.

Received: 20 Jun. 2025
Accepted: 26 Jan. 2026

Editor-in-charge:
Paula Fernanda da Silva Farina